Effect of the Operation of an Electric Motor on the Lengthwise Fracture in the Elements of an Inhomogeneous Mount

Victor Rizov

Department of Technical Mechanics, University of Architecture, Civil Engineering and Geodesy, 1 Chr. Smirnensky blvd., 1046 – Sofia, Bulgaria, E-mail: V_RIZOV_FHE@UACG.BG; ORCID: 0000-0002-0259-3984

https://doi.org/10.29227/IM-2026-02-02-022

Submission date: *2026-10-06* | Review date: *2026-22-06*

Abstract

Technologies applied in modern geotechnics, as well as in mining, frequently use various mechanisms. These mechanisms are often driven by electric motors, which are usually mounted on different types of mounts. Therefore, the reliability and safe operation of mechanisms is directly dependent on the performance of the mounts. The motors generate dynamic loads of the mounts, for example, they cause forced vibrations. This shows that the study of the mechanical behavior and destruction of mounts when they perform forced vibrations is a topical problem. The application of continuously inhomogeneous structural materials of the functionally graded type in mounts under dynamic loading is one of the ways to increase their safety and improve their performance. This paper presents a study of the lengthwise fracture of a continuously inhomogeneous mount with an electric motor mounted on it. The mount represents a structure with two elements. The motor is on the horizontal element of the mount. The rotor of the motor rotates uniformly, which creates a centrifugal force of constant magnitude. The component of this force in the direction of the motor mount vibrations varies according to a harmonic law, which causes forced harmonic vibrations. The horizontal element of the mount is cracked along the length. The main goal of the paper is to obtain a solution of the strain energy release rate (SERR) in mount undergoing forced vibrations. The obtained solution is verified using the method of the integral J. An approach for applying SERR to determine the dimensions of motor mount elements is presented. The approach is visualized with several graphs showing the change in the dimensions when varying various parameters of the mount. This article will contribute to improving the safety of mounts for electric motors.

Keywords: *Mount, Inhomogeneous structure, Dynamic load, Vibration, Lengthwise fracture*

1. Introduction

Geotechnics and mining are important sectors of engineering, which are of great importance for the development of human civilization [1, 2]. For example, the construction of any building structures, transport engineering facilities such as roads, railways, bridges, viaducts, tunnels, ports and airports, hydrotechnical facilities such as dams, canals, pumping stations and reservoirs, various underground facilities such as chambers, storages, machine rooms of hydroelectric power plants, warehouses and others is inextricably linked to the application of geotechnical methods for the design and construction of foundations [3, 4]. In turn, mining provides the necessary resources (energy sources, ore and non-ore minerals, etc.) for the functioning of various industries. All this clearly shows how important it is to work for progress in the field of geotechnics and mining.

However, the development and improvement of modern technologies in geotechnics and mining requires the application of a wide range of machines and mechanisms. In many cases, the mechanisms are driven by electric motors mounted on various types of mounts. This shows that the issues related to the strength, deformability, stability and various forms of failure of motor mounts are of great importance for the safe and reliable functioning of the mechanization used in geotechnics and mining. Therefore, the study of the behavior of mounts under the action of various loads is an important research task with direct practical application in geotechnics and mining. Operating electric motors act on mounts with a force varying in time according to a harmonic law. This force causes forced harmonic vibrations in mounts. This fact shows that ensuring safety is related to studying the failure of mounts performing forced vibrations.

In the context of the above, this paper addresses the problem of lengthwise fracture of mounts with an electric motor mounted on it in a theoretical plan. The mount under consideration is made of a material with continuous inhomogeneity in thickness and length. In this regard, it should be emphasized that continuously inhomogeneous materials have become increasingly popular in recent decades. Typical continuously inhomogeneous materials are functionally gradient ones. They have undergone rapid development since the eighties of the last century [5, 6, 7]. Their very good properties are the main reason for the rapid expansion of their application area. The most characteristic feature of these materials is the smooth change in their mechanical properties, for example, the modulus of elasticity, within the boundaries of a given structural component. However, very often these materials fail as a result of lengthwise cracking (this is due to their layered structure) [8, 9, 10, 11]. This is precisely the reason why we analyze here motor mount in which there is a lengthwise crack. The SERR is determined taking into account the vibrations in the mount. A check with the integral J is made. Graphs are drawn to illustrate some applications of SERR.

2. Analysis of the Motor Mount

The motor mount studied here has two elements, namely B_1B_5 and B_4B_6 (Fig. 1). The element, B_1B_5, is supported at points, B_1 and B_5. The element, B_4B_6, is supported at point, B_6. Due to the inhomogeneity of the material, the modulus of elasticity, E, varies continuously both along the thickness and length of the mount elements. An electric motor is mounted on the

mount at point, B_3. The dead weights of the stator and rotor are G_S and G_R, respectively. The rotor performs n_R revolutions per minute. The arm (eccentricity) of the rotor mass is r.

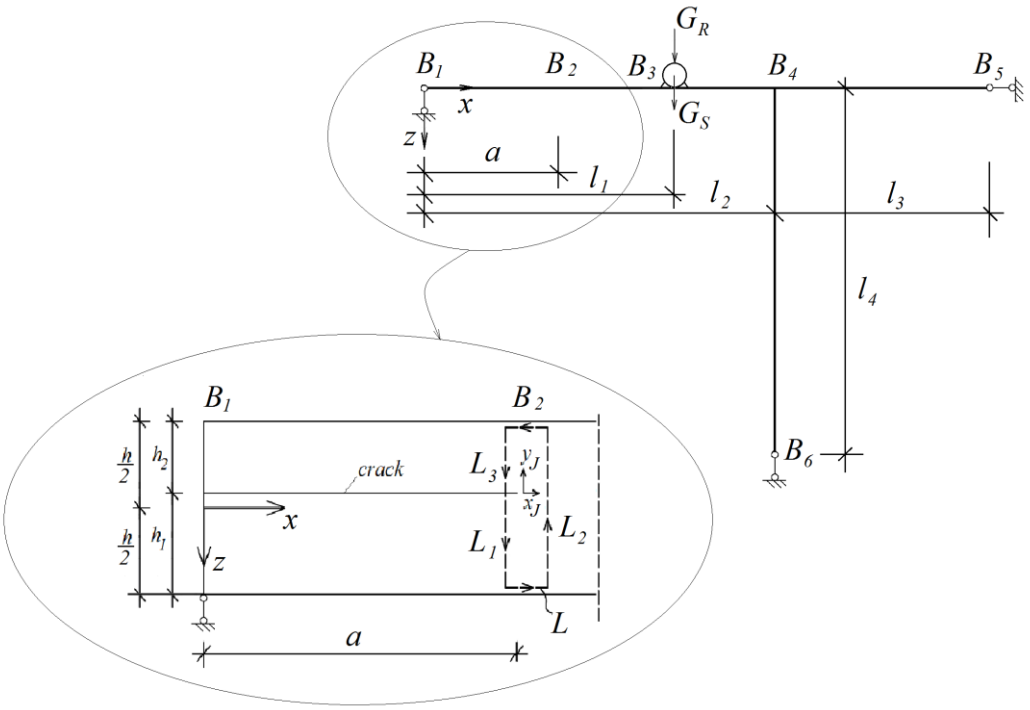

Fig. 1. Mount with an electric motor.

SERR, G_{st}, for the lengthwise crack in a section, B_1B_2, of element, B_1B_5, from the static action of G_S is

$$G_{st} = \frac{1}{b}\left(G_S \frac{\partial w_{B_3}}{\partial a} - \frac{\partial U}{\partial a} \right). \tag{1}$$

In (1) the following notations are introduced: b - width of the mount elements (refer to Fig. 2); a - length of the lengthwise crack; w_{B_3} - displacement of point, B_3, in the direction of action of G_S; U - strain energy in the mount.

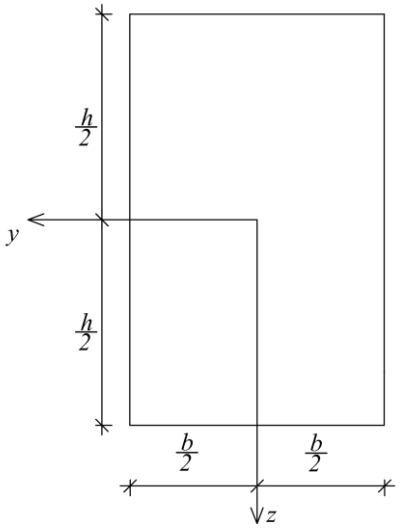

Fig. 2. Dimensions of the motor mount elements.

Dependence (1) is a result of considering the change in energy with a small increase in the crack length. The aforementioned consideration is written as

$$G_S \delta w_{B_3} = \frac{\partial U}{\partial a}\delta a + G_{st} b \delta a\,, \tag{2}$$

from which dependence (1) is obtained.

The displacement, w_{B_3}, is

$$w_{B_3} = \sum \int \kappa_i M_i dx. \tag{3}$$

The notations in (3) are: κ_i – curvature of the element; M_i – moment of the unit load; x - longitudinal axis.

The strain energy is

$$U = U_{lw} + U_{up} + U_{B_2B_3} + U_{B_3B_4} + U_{B_4B_5} + U_{B_4B_6}, \tag{4}$$

where

$$U_{lw} = \iiint\limits_{(V_{lv})} u_{0lw} dV, \tag{5}$$

$$U_{up} = \iiint\limits_{(V_{up})} u_{0up} dV, \tag{6}$$

$$U_{B_2B_3} = \iiint\limits_{(V_{B_2B_3})} u_{0B_2B_3} dV, \tag{7}$$

$$U_{B_3B_4} = \iiint\limits_{(V_{B_3B_4})} u_{0B_3B_4} dV, \tag{8}$$

$$U_{B_4B_5} = \iiint\limits_{(V_{B4B_5})} u_{0B_4B_5} dV, \tag{9}$$

$$U_{B_4B_6} = \iiint\limits_{(V_{B_4B_6})} u_{0B_4B_6} dV. \tag{10}$$

The following notations are introduced in formulas (5) – (10): u_{0lw} and u_{0up} - specific strain energies in the lower and upper arm of the crack; $u_{0B_2B_3}$, $u_{0B_3B_4}$, $u_{0B_4B_5}$ and $u_{0B_4B_6}$ - specific strain energies in elements, B_2B_3, B_3B_4, B_4B_5 and B_4B_6, of the mount.

u_{0lw} is found with the following sequence of formulas:

$$u_{0lw} = \frac{1}{2}\sigma\varepsilon, \tag{11}$$

$$\sigma = E\varepsilon, \tag{12}$$

$$\varepsilon = \kappa_1(z_1 - z_{1n}), \tag{13}$$

$$E = E_{vz} e^{\theta\frac{\frac{h}{2}+z}{h}}, \tag{14}$$

$$E_{vz} = E_{vz0} e^{\psi\frac{x}{l_2+l_3}}, \tag{15}$$

where

$$-\frac{h_1}{2} \le z_1 \le \frac{h_1}{2}, \tag{16}$$

$$-\frac{h}{2} \le z \le \frac{h}{2}, \tag{17}$$

$$0 \le x \le l_2 + l_3. \tag{18}$$

In (11) – (18) the following notations are used: σ - stress; ε - strain; E - modulus of elasticity; z_{1n} - distance of the zero line from the center; z_1 - centric axis of the lower arm of the crack; θ and ψ - parameters of distribution of E along the thickness and length of the elements of the mount; z - axis; h, h_1, l_2 and l_3 - parameters of the mount geometry shown in Fig. 1.

To find κ_1 and z_{1n} we use MatLab. We apply the equations

$$N = \iint_{(A_1)} \sigma dA, \tag{19}$$

$$M = \iint_{(A_1)} \sigma z_1 dA, \tag{20}$$

where

$$A_1 = bh_1. \tag{21}$$

The following notations are introduced in the above equations: N - axial force; M - bending moment; b - width of the element.

The logic by which we find u_{0up}, $u_{0B_2B_3}$, $u_{0B_3B_4}$, $u_{0B_4B_5}$ and $u_{0B_4B_6}$ is the same as that for finding u_{0lw}. After finding u_{0lw}, u_{0up}, $u_{0B_2B_3}$, $u_{0B_3B_4}$, $u_{0B_4B_5}$ and $u_{0B_4B_6}$, we move on to determining U_{lw}, U_{up}, $U_{B_2B_3}$, $U_{B_3B_4}$, $U_{B_4B_5}$, $U_{B_4B_6}$, U, and G_{st} using formulas (5) – (10), (4) and (1), respectively.

The SERR in the mount from the rotor centrifugal force is denoted by G_{dyn}. The logic by which we determine G_{dyn} is similar to that for G_{st}. This means that we must replace the force, G_S, with the centrifugal force, P, in the formulas for SERR from the static action of G_S.

The centrifugal force is

$$P = \omega_R^2 r \frac{G_R}{g}, \tag{22}$$

where

$$\omega_R = \frac{\pi n_R}{30}. \tag{23}$$

The vertical component of P represents a harmonic force that causes vibrations in the motor mount.

The dynamic stresses and strains, σ_{dyn} and ε_{dyn}, from P are

$$\sigma_{dyn} = k_{dyn}\sigma, \tag{24}$$

$$\varepsilon_{dyn} = k_{dyn}\varepsilon, \tag{25}$$

where [12]

$$k_{dyn} = \frac{1}{\left|1 - \frac{\omega_R}{\omega}\right|}, \tag{26}$$

$$\omega = \sqrt{\frac{g}{w_{B_3}}}. \tag{27}$$

It is the dynamic stresses and strains that are used in finding G_{dyn}.

Of primary interest is the highest SERR. It is

$$G = G_{st} + G_{dyn}. \tag{28}$$

We check SERR through the integral J, solved with MatLab. First we check G_{st}. Using the contour, L, we obtain (Fig. 1) [13].

$$J_{st} = J_{stL_1} + J_{stL_2} + J_{stL3}, \tag{29}$$

where

$$J_{stL_1} = \int \left[u_{0L_1} \cos\alpha_{L_1} - \left(p_{x_J L_1} \frac{\partial u}{\partial x_J} + p_{y_J L_1} \frac{\partial v}{\partial x_J} \right) \right] ds_{L_1}, \tag{30}$$

$$J_{stL_2} = \int \left[u_{0L_2} \cos\alpha_{L_2} - \left(p_{x_J L_2} \frac{\partial u}{\partial x_J} + p_{y_J L_2} \frac{\partial v}{\partial x_J} \right) \right] ds_{L_2}, \tag{31}$$

$$J_{stL_3} = \int \left[u_{0L_3} \cos\alpha_{L_3} - \left(p_{x_J L_3} \frac{\partial u}{\partial x_J} + p_{y_J L_3} \frac{\partial v}{\partial x_J} \right) \right] ds_{L_3}. \tag{32}$$

The elements of J_{stL_1} are

$$u_{0L_1} = \int \sigma d\varepsilon, \tag{33}$$

$$\cos\alpha_{L_1} = -1, \tag{34}$$

$$p_{x_J L_1} = -\sigma, \tag{35}$$

$$\frac{\partial u}{\partial x_J} = \varepsilon, \tag{36}$$

$$p_{y_J L_1} = 0. \tag{37}$$

The logic by which we find the elements of J_{stL_2} and J_{stL_3} is similar to that for J_{stL_1}.

We also check G_{dyn}. The logic for obtaining the solution of J_{dyn} is similar to that for J_{st}. The only difference is that we use the dynamic stresses and strains from the action of P.

The integrals, J_{st} and J_{dyn}, correspond exactly to G_{st} and G_{dyn}.

3. Dimensioning of the Motor Mount

The above theoretical analysis of SERR can be applied to the dimensioning of the elements of a motor mount. More precisely, an application of the SERR solution to determine the thickness of the elements is considered here.

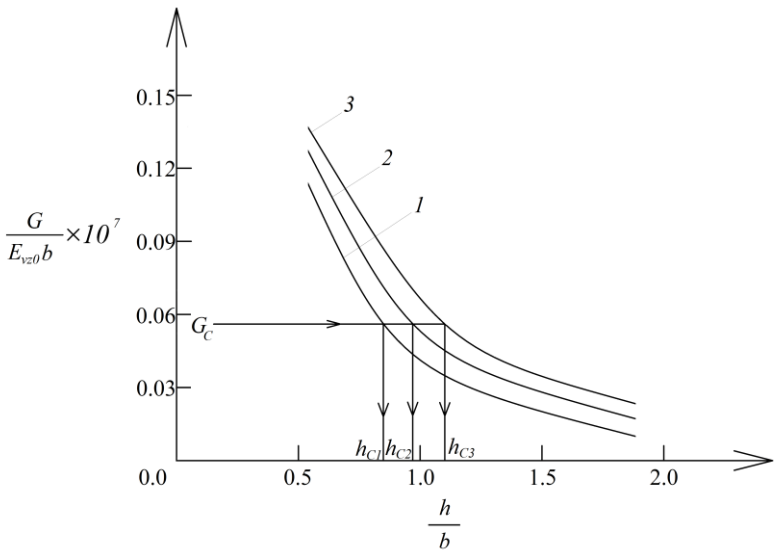

Fig. 3. Determination of the required thickness of the elements for $\omega_R / \omega = 0.15$ (curve 1), $\omega_R / \omega = 0.30$ (curve 2) and $\omega_R / \omega = 0.45$ (curve 3).

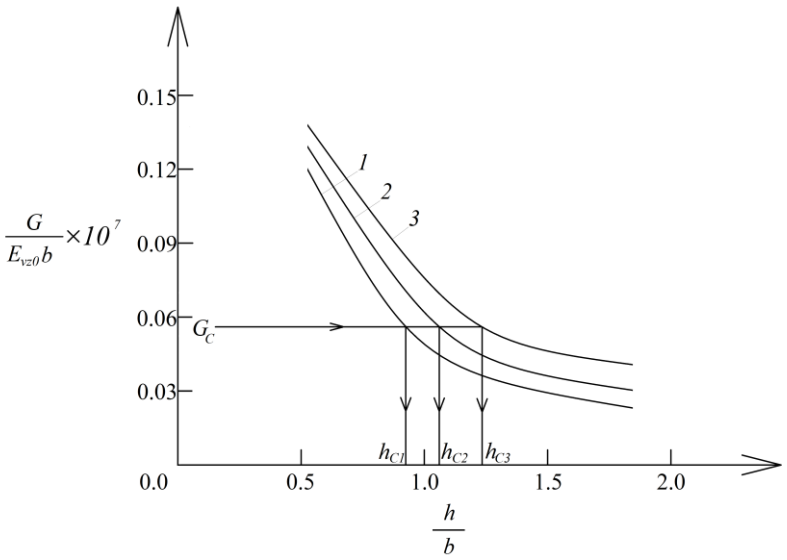

Fig. 4. Influence of the ratio l_2 / b on the required thickness of the elements ($l_2 / b = 15$ - curve 1, $l_2 / b = 25$ - curve 2 and $l_2 / b = 30$ - curve 3).

The application is based on the principles of fracture mechanics. It is studied how the thickness of the mentioned elements depends on the frequency of the harmonic force with which the electric motor acts on the mount. The dependence of the thickness on the length of the crack and on the length of the element, B_1B_4, is also analyzed. The following numerical data are used: $b = 0.150$ m, $l_1 = 1.500$ m, $l_2 = 3.000$ m, $l_3 = 1.800$ m, $l_4 = 2.500$ m, $a = 1.300$ m, $\theta = 1.5$ and $\psi = 2.0$.

First, it is studied how the thickness of the elements can be determined at different frequencies of the harmonic force. The thickness is found by the equation

$$G = G_C, \quad (35)$$

where G_C is the fractional toughness. In principle, (35) is a criterion for the growth of the longitudinal crack, i.e. the thickness, h_C, is found from the condition of not allowing the crack to grow. The determination of the thickness is shown in Fig. 3 for three ratios, ω_R / ω. The conclusion that follows from the graphs in Fig. 3 is that the increase in the ratio, ω_R / ω, has a negative effect on the lengthwise fracture behavior of the mount, because the SERR increases, which in turn determines the increase in the required thickness, h_C. In other words, greater ω_R / ω leads to the need to use thicker mount elements.

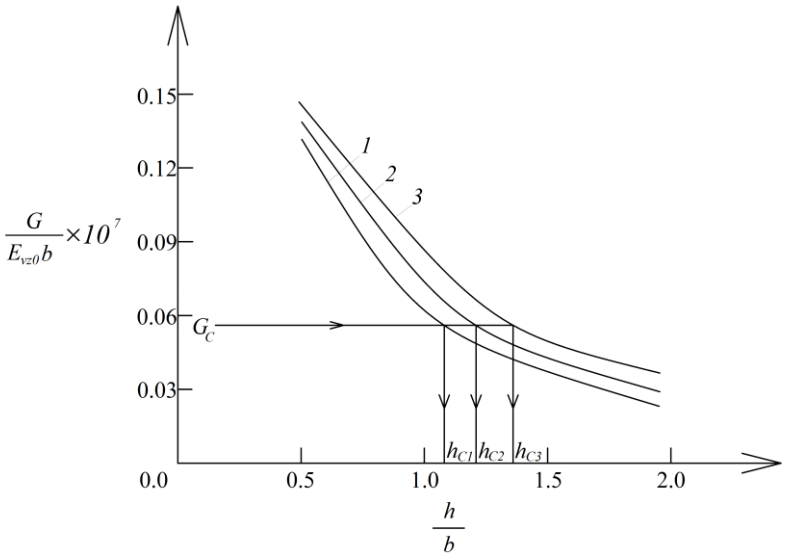

Fig. 5. Effect of the ratio, a / l_1, on the required thickness of the elements ($a / l_1 = 0.3$ - curve 1, $a / l_1 = 0.6$ - curve 2 and $a / l_1 = 0.9$ - curve 3).

The determination of the thickness at different lengths of the element, B_1B_4, is illustrated by the graphs in Fig. 4. The length of the element, B_1B_4, is represented in a dimensionless form by the ratio, l_2/b. The conclusion from the graphs in Fig. 4 is that the greater length of B_1B_4 leads to higher SERR, which determines the obtaining of a larger required thickness, h_C.

Finally, we will focus on the determination of the thickness of the mount elements at different ratios, a/l_1. In this regard, the graphs in Fig. 5 are drawn. An examination of the graphs shows that higher values of the ratio, a/l_1, lead to higher SERRs, which is the reason for the greater required thickness of the elements.

4. Conclusion

A theoretical analysis of the lengthwise fracture of a mount with an electric motor on it is presented. The mount elements are made of continuously inhomogeneous material in thickness and length. As a result of the analysis, SERR was obtained. The influence of the mount vibrations due to the operation of the electric motor was taken into account. A check was made with the J integral. The main emphasis in this work is placed on the practical application of SERR for sizing the motor mount elements. The determination of the required thickness of the elements is presented in detail, applying the condition not to allow the growth of the existing lengthwise crack during forced vibrations of the mount. It is considered how the required thickness is determined taking into account the effect of the ratios, ω_R/ω, l_2/b, and a/l_1. As a result, it is established how these ratios affect the required thickness. The results, illustrated with relevant graphs, show that increasing these ratios requires the use of elements with greater thickness (the reason for this is the increase in SERR). The present work can be developed in the direction of studying the lengthwise fracture of the elements of a spatial mount during vibrations caused by the operation of an electric motor. This will require performing a more complex analysis taking into account the torsion of the motor mount elements.

References

1. G. Stefanov, Handbook of geotechnics – Part 1 (Technique, 1989).
2. G. Stefanov, Handbook of geotechnics – Part 2 (Technique, 1989).
3. V. Venkov, Retaining walls and structures (Technique, 1982).
4. N. Citovich, Geomechanics (Science, 1983).
5. Q. Du, X. Jin, W. Farid, and H. Yu, “Fabrication Methodologies of Functionally Graded Materials: Advances, Performance Regulation, and Future Perspectives”, Advanced Materials Technologies 11, e01864 (2026).
6. Y. Li, Z. Feng, L. Hao, L. Huang, C. Xin, Y. Wang, E. Bilotti, K. Essa, H. Zhang, Z. Li, F. Yan and T. Peijs, “A Review on Functionally Graded Materials and Structures via Additive Manufacturing: From Multi-Scale Design to Versatile Functional Properties”, Adv. Mater. Technol, 5, 1900981 (2020).
7. G. D. S. Rakshith, K. K. J. Hemanth and L. R. Jyothi. “Fabrication Methods of Functionally Graded Materials—A Review”, Advances in Mechanical Engineering and Material Sciences, 288-294 (2026).
8. N. A. Dolgov, “Analytical Methods to Determine the Stress State in the Substrate – Coating System Under Mechanical Loads”, Strength of Materials 48, 658-667 (2016).
9. N. Dowling, S. Kample and M. Kral, Mechanical Behavior of Materials: Engineering Methods for Deformation, Fracture, and Fatigue (5th Edition, Pearson, 2019).
10. V. Rizov, “Analysis of delamination in moving systems “multilayered beam – particle”, Strength, Fracture and Complexity, (2025).
11. V. Rizov, “Longitudinal Fracture Analysis of Continuously Inhomogeneous Beams Undergoing General Planar Motion”, J. Appl. Comput. Mech., 12, 111-123 (2026).
12. V. Alexandrov and V. Nedev, Strength of materials (TU, 2005).
13. D. Broek, Elementary engineering fracture mechanics (Springer, 1986).